Article

Techno-Economic Aspects of Noble Gases as Monitoring Tracers

Ulrich Wolfgang Weber [1,*] , Niko Kampman [2] and Anja Sundal [1]

[1] Department of Geosciences, University of Oslo, 0371 Oslo, Norway; anja.sundal@geo.uio.no
[2] Shell Global Solutions International B.V., 1031 Amsterdam, The Netherlands; niko.kampman@shell.com
* Correspondence: u.w.weber@geo.uio.no; Tel.: +47-939-61-506

Abstract: A comprehensive monitoring program is an integral part of the safe operation of geological CO_2 storage projects. Noble gases can be used as geochemical tracers to detect a CO_2 anomaly and identify its origin, since they display unique signatures in the injected CO_2 and naturally occurring geological fluids and gases of the storage site complex. In this study, we assess and demonstrate the suitability of noble gases in source identification of CO_2 anomalies even when natural variability and analytical uncertainties are considered. Explicitly, injected CO_2 becomes distinguishable from shallow fluids (e.g., subsea gas seeps) due to its inheritance of the radiogenic signature (e.g., high He) of deep crustal fluids by equilibration with the formation water. This equilibration also results in the CO_2 inheriting a distinct Xe concentration and Xe/noble gas elemental ratios, which enable the CO_2 to be differentiated from deep crustal hydrocarbon gases that may be in the vicinity of a storage reservoir. However, the derivation has uncertainties that may make the latter distinction less reliable. These uncertainties would be best and most economically addressed by coinjection of Xe with a distinct isotope ratio into the CO_2 stream. However, such a tracer addition would add significant cost to monitoring programs of currently operating storage projects by up to 70% (i.e., from 1 $US/t to 1.7 $US/t).

Keywords: carbon capture and storage; monitoring and verification; noble gases; leakage detection; inherent distinctiveness; tracer addition; cost calculation

1. Introduction

Measurement, monitoring, and verification (MMV) programs are an essential part of the safe operation of geological CO_2 storage (GCS or CCS, when including capture) project [1,2]. On the one hand, a robust MMV strategy helps to ensure long-term storage security, to meet climate change mitigation goals, and to manage public acceptance [1]. On the other hand, for scaling CCS to climate relevant amounts of CO_2 stored, the associated cost of such a strategy cannot jeopardize the economic viability of a project that is heavily dependent on carbon pricing [3].

Chemical changes and tracers can be monitored at storage sites, potentially enabling detection of a CO_2 leak and identification of the source of observed anomalies [1,4]. Noble gases are one chemical tracer group that has received attention due to their key properties of being inert and having a large number of isotopes that can be measured with high precision [5,6]. This makes them safe to utilize in industrial processes and their use does not have additional negative environmental consequences. The concentrations of He, Ne, Ar, Kr, Xe, and their isotopic ratios constitute the noble gas signature of a fluid. This practically labels most environmental reservoirs with an identifiable atmospheric [7], crustal (radiogenic) [8], or mantle [9] signature [10]. Further, injected CO_2 from various capture processes (anthropogenic) has an inherent noble gas signature, which depends on the CO_2 source and capture process [11–13].

The conservative behavior of noble gases and the knowledge of the baseline noble gas signatures of the storage system allows end-member mixing calculations to be performed, such as those used in a study that refused an alleged leak from a CO_2 storage site [14].

Further, in CO_2 injection for enhanced oil recovery (EOR), changes in the noble gas signature of the produced fluids quantified the contribution of the injected CO_2 [15–17]. It is also possible to label the injected CO_2 with deliberately added noble gases to distinguish the signature of the injected CO_2 further [15,18]. However, this has only been conducted in small-scale injection experiments, but allowed for identification of the CO_2 gas plume distribution and of mixing and degassing processes, e.g., [19].

In the study by Roberts et al. [18], the addition of noble gas tracers is discussed from a practicality and cost perspective for large-scale storage. Tracer addition was analyzed to differentiate the noble gas signature of the injected, and eventually, leaking CO_2 from the background signatures of seawater and atmosphere. They conclude that He and ^{124,129}Xe isotopes are most suitable as added tracers with costs in the order of 100–100,000 £/$MtCO_2$, similar to earlier results by Nimz et al. [15].

In [12,13], we outlined that the injected CO_2 is likely to inherit a radiogenic noble gas signature from the storage formation waters through equilibration or mixing with native formation gases. The calculation based on phase partitioning data for a high-pressure CO_2-H_2O-system [20] led to the hypothesis that injected CO_2 becomes differentiable from atmospheric signatures without the need of adding tracers.

The altered, radiogenic signature of the injected CO_2 is similar to natural hydrocarbons [21]. Hydrocarbon reservoirs are often found in the vicinity of a number of active or suggested CO_2 storage sites, e.g., [22–24]. A leak into such hydrocarbon reservoirs may not have the environmental impact of a leak to the seabed, but the contamination of these resources can have significant economic consequences. Further, if the CO_2 was to be fed back into the atmosphere, subsequent to gas or oil production, the climate mitigation value of a CCS project would be reduced. Therefore, there is the need to expand the evaluation of the distinctiveness of noble gas signatures and tracer addition to include the discrimination of CO_2 and hydrocarbon gases.

There are several possible scenarios of how leakage could occur to the atmosphere or seabed or into hydrocarbon reservoirs [25]. An overview of some possible pathways that may result in varying exchange of the injected CO_2 with the storage site fluids and mixture with different background reservoirs is shown in Figure 1. An injection well leak, case 1 in Figure 1, could leave the CO_2 with its initial composition; meanwhile, cases 2, 3, 4, and 5 would likely lead to significant interaction of the CO_2 with crustal fluids. Therefore, including the phase partitioning between the injected CO_2 and formation water data derived in [20] is an essential addition in the assessment of noble gas tracers, both from a technical and economic perspective.

In this work, we aim to validate the hypothesis of the inherent differentiability of the injected CO_2 from the atmospheric signatures quantitatively drawn in [12]. We will conduct calculations based on current analytical capabilities for noble gases and the natural variability of noble gas signatures. In the same way, we evaluate distinctiveness to other environmental signatures, i.e., natural gas and gas hydrates, that have to be considered in the leakage scenarios 2–5 in Figure 1. Then, we derive the necessary amounts and the associated cost for tracer addition to increase distinctiveness between the injected CO_2 and hydrocarbons, i.e., natural gas. Finally, we discuss the practical and economic roles of noble gases in a monitoring scheme and the implications for the viability of a storage project.
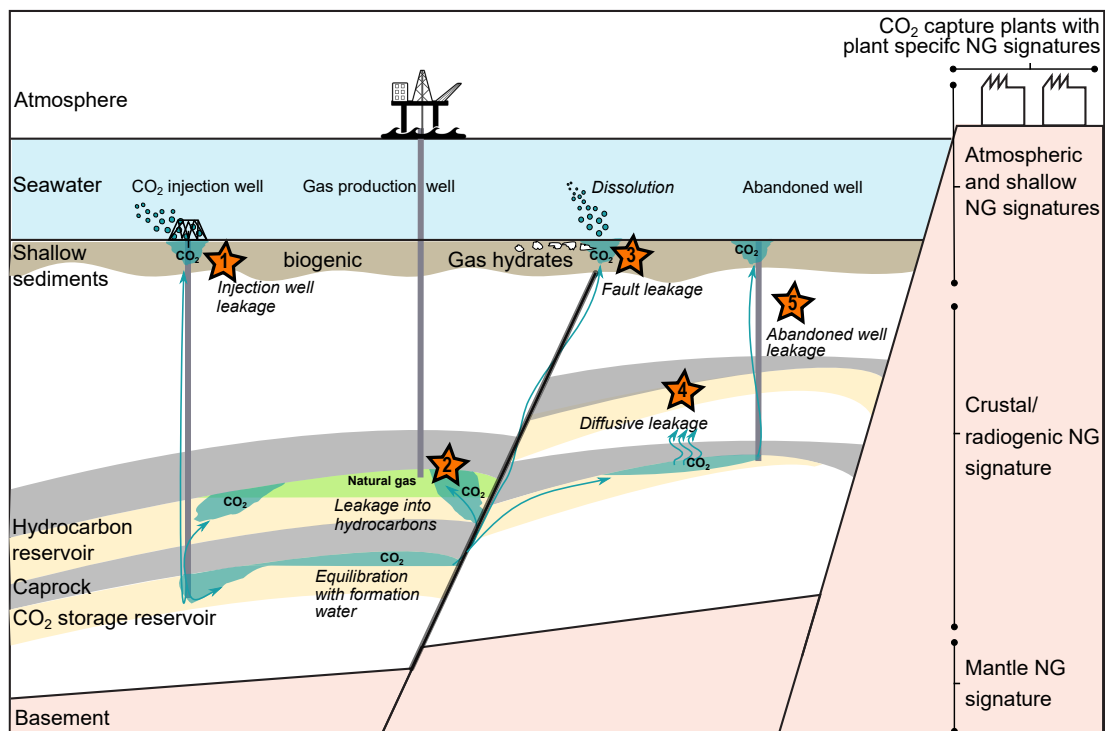
Figure 1. Overview sketch of a CO_2 storage site with areas typically attributed to a type of noble gas (NG) signature [10]. CO_2 will have a different NG signature for different plant types, such as postcombustion, natural gas processing, or oxyfuel [11,12]. Possible leakage pathways are (1) injection well leakage, (2) migration into and contamination of hydrocarbon reservoirs that may subsequently be produced, (3) fault leakage, (4) diffuse leakage, and (5) leakage through an abandoned well. Leaking CO_2 may enter the atmosphere or dissolve in seawater.

2. Materials and Methods

2.1. Background Concentrations

Noble gas tracers have widespread application in deciphering physical and chemical processes in geosciences [10] since they are only influenced by physical processes. There are three main groups of noble gas signatures in the environment, which are of atmospheric [7], crustal [8], or mantle [9] character and allow researchers to attribute the source of a fluid. In practice, these categories in themselves can have wide isotopic concentration ranges or be mixtures derived during the history of origin of a fluid. Characterizing the background fluids of a storage site is key for the applicability of noble gases as tracers.

Here, we collect and discuss the known signatures from samples relevant to a possible storage site in the North Sea (Table 1). This is due to the topicality of the Norwegian large-scale storage project 'Longship', which is currently under development [26]. Additionally, in this project, a contamination of the stratigraphically overlying Troll gas and oil field could be considered a risk [27]. Analogue studies may be used and discussed where samples are not available. These signatures may have to be adapted for other sites but reflect typical continental shelf settings.

For natural gas, sample analyses for the North Sea are currently available for the Sleipner Vest and the Magnus fields [28,29]. The results show a typical crustal, radiogenic character, derived from the accumulation of ^{4}He, ^{21}Ne, and ^{40}Ar through radioactive decay of the elements K, U, and Th in the rocks [8]. The radioactive accumulation is a function of time and the content of radioactive elements in the rock. The radiogenic signature acquires an atmospheric gas component from the in situ formation water that was in atmospheric equilibrium during sedimentation, or meteoric recharge. The additional amounts of stripped gas then depend on the gas/water volume ratio, V_g/V_w, and if the hydrocarbon system is closed or open, allowing for significant gas volumes to migrate through a reservoir [28].

Table 1. Observed noble gas concentrations for different environmental fluids. Natural gas for He, Ne, and Ar compiled from the North Sea Sleipner and Magnus Fields in [28,29], and Kr and Xe from the Sleipner Field [28]. Natural, geologic CO_2 compiled from [30,31]. Sediment values from the South Pacific Ocean [32] and the Mediterranean Ridge for He [33]. Gas hydrates from [34]. Seawater concentrations after [35] (assuming a temperature of 7.5 °C and a salinity of 34.2 g/L). Atmospheric values from [7]. Captured CO_2 from several sites [11–13]. In cm^3_{STP}/cm^3_{STP}, if not otherwise stated. Rounded to nearest tenth asides atmosphere.

	He	Ne	Ar	Kr	Xe
Natural Gas/Oil	1.2E-05–1.3E-04	7.0E-07–2.7E-08	1.1E-05–4.1E-05	4.1E-09–5.2E-09	1.3E-09–1.6E-09
Natural, geologic CO_2	1.0E-04–1.0E-02	7.0E-08–1.8E-06	1.5E-05–2.7E-05	1.0E-10–1.0E-08	5.0E-12
Gas Hydrates	7.0E-10–9.0E-10	2.5E-09–6.2E-08	3.5E-05–5.3E-04	1.8E-08–3.0E-07	2.7E-09–9.4E-08
Seafloor Sediments (cm^3_{STP}/g)	1.0E-04–1.0E-02	5.0E-09–5.0E-07	1.0E-05–1.0E-08	5.0E-08–1.5E-09	8.0E-09–1.7E-08
Seawater (cm^3_{STP}/g)	4.0E-08	5.7E-09	1.1E-06	8.5E-08	1.1E-08
Atmosphere	5.24E-06	1.82E-05	9.34E-03	1.13E-06	8.7E-08
Captured CO_2	2.3E-09–2.9E-06	5.9E-11–4.3E-07	3.7E-10–1.4E-04	3.6E-12–6.3E-09	1.1E-13–1.9E-09

Natural, geologic CO_2 shows dominantly magmatic, and hence, mantle signatures with subsequent equilibration with radiogenic formation water. The values in Table 1 are from large natural CO_2 systems in the US [30,31]. Natural CO_2 in the North Sea context is typically a minor constituent of natural gas accumulations, e.g., [22], and would therefore have very similar noble gas signatures as the associated hydrocarbons.

The values for both natural gas and natural, geologic CO_2 depict that the noble gas concentration within what is considered a radiogenic signature can vary by orders of magnitude (see Table 1). For the 'Longship' project, the most relevant radiogenic signature to compare to with respect to traceability of CO_2 is storage reservoir formation water and gas and oil in the Troll Field stratigraphically overlying the storage formation. Even though the Troll gas and oil reservoirs are shallower than in the Magnus and Sleipner fields, the age and the proposed origin of the Troll hydrocarbons in the Oseberg area [36] would suggest that noble gas signatures in the Troll field are similar to those in Table 1.

Close to the seabed, gas hydrates may occur. Only total gas concentration, not isotopic composition, have been analyzed for these [34]. Those samples were collected outside the coast of Oregon, US, and showed a quite specific fractionation pattern with preferential incorporation of heavier noble gases and suppression of the lighter ones. This fractionation process should be independent of the location, making the concentrations applicable for the North Sea if gas hydrates were to be found.

Analysis of the dissolved noble gas distribution in the pore-water of shallow, unconsolidated sediments are relatively rare [32,33,37] and, for the North Sea, there is no dataset available. Sediment pore-water concentrations are dependent on the temperature during sedimentation and if there are leakage sites, e.g., shallow biogenic gas or deep fluid release, such as black smokers, nearby. The data from [32,33,37] in Table 1 has to be seen in the context of plate boundaries and is therefore not representative for the continental crust of the North Sea. However, there have been methane leakages above the Troll field in the past [38], which could have left a minor radiogenic component in the pore-water signature.

Seawater, if not in the vicinity of specific fluid releases, is typically air equilibrated water at a given temperature and salinity [35]. This means atmospheric gas, including noble gases, is dissolved based on the solubility of the respective gas species at these conditions in water. In case there are seepages, ocean currents may redistribute them quickly, so anomalies can be local. The atmosphere is typically well mixed and has a specific noble gas signature [7].

The noble gas signature of captured CO_2 has been analyzed for several capture plants in Norway [12,13] and other countries [11]. Noble gas concentrations are typically low and the isotopic signatures are either airlike for plants with combustion prior to capture (e.g., waste incineration) or natural-gas-like (e.g., natural gas processing). For captured CO_2,

the observed range spans several orders of magnitude. Captured CO_2 from oxyfuel plants, for example, are significantly enriched in Kr and Xe [6].

With regards to isotopic ratios, there are the three main signatures and fluids that represent mixtures of these to various degrees. Typical values for the mainly affected isotopes are shown in Table 2.

Noble gas ratios associated with hydrocarbons are, as previously discussed for concentrations, dependent on the geological setting of a reservoir and the provenance of the hydrocarbons. In Table 2, isotopic ratios are shown for the North Sea [28]. However, the ^{3}He/^{4}He and ^{40}Ar/^{36}Ar ratio especially can vary significantly, e.g., natural gas from Snøhvit has a He-ratio an order of magnitude lower [12].

Table 2. Isotopic ratios for the main signatures: atmospheric; crustal, hence radiogenic; and mantle. Atmospheric values from [7]. Natural gas from the Sleipner field [28]. Mantle data from [9].

	^{3}He/^{4}He (R/R$_A$)	^{21}Ne/^{22}Ne	^{40}Ar/^{36}Ar	^{86}Kr/^{84}Kr	^{132}Xe/^{130}Xe
Atmospheric Signature	1	0.029	296	0.303	6.61
Crustal signature	~0.1	~0.033	~455	~0.303	~6.61
Mantle signature (MORB)	8	0.06	~30,000	-	-

For captured CO_2, the ratios are dependent on the source of the CO_2 and if combustion has taken place prior to capture, e.g., at heat and power plants. Combustion introduces noble gases from the air shifting ratios towards atmospheric values. At natural gas processing sites, the radiogenic ratios are maintained [12]. However, one has to consider that the CO_2 can undergo interaction with, for example, in situ formation water or gases, subsequently altering the noble gas fingerprint, as we discuss next.

2.2. Phase Partitioning

Following injection, the equilibration of the injected CO_2 with the formation water of the storage reservoir will significantly modify its composition, especially given that captured and injected CO_2 will be significantly depleted in noble gases [12]. We calculate this phase partitioning by applying Henry's law following the derivation for the thermodynamic conditions governing in the crust in [39]. The gas concentration c of a gas i in the gas phase calculates to

$$c_{i,g} = c_{i,T} \left(\frac{22400 T \rho_{H_2O}}{18 \cdot 273 \frac{\gamma_i}{\phi_i} K_{i,CO_2-H_2O}} \frac{V_{H_2O}}{V_{CO_2}} + 1 \right)^{-1}, \tag{1}$$

with the total concentration c_T of gas i; water density ρ_{H_2O} at system pressure; temperature T; activity γ_i; and fugacity ϕ_i of the gas at system pressure, temperature, and volume of water CO_2, V_{H_2O}, and V_{CO_2}, respectively.

Values of K_{i,H_2O}, γ_i, and ϕ_i are collected in [39]. However, Henry's constants K_i of noble gases were found to deviate significantly for a high-density CO_2-H_2O system [20]. Warr et al. [20] experimentally derived deviation factors κ_i for all noble gases besides Ne and Rn. This correction allows calculation of the deviation of Henry's constant with gas-specific constants in the dependency of CO_2 density:

$$K_{i,CO_2-H_2O} = \kappa_i K_{i,H_2O} = \left(\frac{a_i \rho_{CO_2}^2 + b_i \rho_{CO_2} + c_i}{100} + 1 \right) K_{i,H_2O}. \tag{2}$$

K_{i,H_2O} is Henry's constant at a given temperature in units of pressure for a low-pressure air–water system. The upper limit for density in the experiments of [20] was 656 kg/m^3. Though explicitly advised against, we also apply this deviation for densities up to 700 kg/m^3 due to the lack of data.

The densities in Equations (1) and (2) are also functions of temperature and pressure, which can be expressed as gradients of depth. Geothermal and pressure gradients vary in different geological settings. Here, we use 30 K/km and 10.18 MPa/km. We derive the densities for CO_2 from [40] and for H_2O from [41].

Since Equation (1) is a function of the volume ratio V_{H_2O}/V_{CO_2}, phase partitioning can be calculated independent of actual storage site volume. In this work, we derive phase-partitioned values at the ratio of maximum saturation S_{max} of CO_2 for residual trapping in a reservoir rock containing CO_2 and water. The CO_2 saturation was found experimentally to be between 13 and 92% for several reservoir rock samples, with a mean of 61% [42], which is subsequently used.

The total concentration of a gas in the system is derived from the sum of the product of concentration in the single phases and their volumes, hence,

$$c_{i,T} = c_{i,CO_{2,inj}} \cdot V_{CO_2} + c_{i,H_2O} \cdot V_{H_2O}, \tag{3}$$

where $c_{i,CO_{2,inj}}$ are the inherent concentrations in captured CO_2 (see Table 1). There are currently no formation water analyses on noble gases for the North Sea. Therefore, we derive the formation water concentrations, c_{i,H_2O}, assuming natural gas from the Sleipner field in [28] had been in equilibrium with formation water. For the calculation of tracer addition, the concentrations in $c_{i,CO_{2,inj}}$ can be altered such that Equation (1) results in the desired $c_{i,g}$.

2.3. Distinctiveness

The distinctiveness of the noble gas signature is constrained by analytical capabilities and natural variability. These have to be considered when analyzing the reliability of mixing calculations. In [18], it is assumed that "10 times the detectable perturbation above background levels are required for reliable tracer detection in the atmosphere or seawater", hence, a leak would then be identified. As discussed in Section 2.1, the signatures in the atmosphere and seawater that were analyzed in [18] can be reasonably assumed to be fixed.

Tables 1 and 2 show that this is not the case for hydrocarbons and gas hydrates, such that the natural variability has to be considered to further constrain the distinctiveness. We use the values in [28] to derive the natural variability that can be expected for a gas field. The resulting ranges are smaller than observed in the Magnus Field [29]; however, it appears that analytical capabilities have increased significantly, such that the samples from [28] are likely to reflect state-of-the-art precision and accuracy.

Our criterion for being distinct is that the resulting concentration in a mixture of 90% background fluid and 10% equilibrated CO_2 has to be larger than the natural variability plus the 3σ-interval of the typical measurement error in [28].

3. Results

3.1. Equilibration with Formation Water

The phase partitioning of injected CO_2 with the formation water leads to a significant change of the initially depleted signature of the captured CO_2. The results of the calculation at 2000 m depth following Section 2.2 for the respective isotopes and ratios are shown in Table 3. Ne is not further considered since there are no correction terms for a CO_2-H_2O-system available.

Injected CO_2 acquires a specific signature. With the high He ($\sim$3.90E-05 cm^3_{STP}/cm^3_{STP}), it may be considered a radiogenic signature; however, the correction term for the solubilities for a CO_2-H_2O-system (Equation (2)) affects each gas species individually. For example, the phase partitioning leads to a signature that is $\sim$500% different compared to natural gas in Xe. It is also very different compared to atmosphere, $\sim$750% in He, and compared to gas hydrates $\sim$5E+07% in He Table 3.

Results are calculated both for the highest and lowest values in captured CO_2 (see Table 1). The concentrations in the injected CO_2 are most influential for Ar results with a resulting $\sim$50% difference for ^{36}Ar.

These values can be compared to the analytical uncertainty of an elements measurement and the natural variability in natural gas for the results of the Sleipner field [28], which can be as high as 45%, as stated in Table 3.

Table 3. Noble gas concentrations in cm_{STP}^3/cm_{STP}^3 and isotopic ratios after equilibration with formation water for low and high concentrations in captured CO_2, as in Table 1. Analytical uncertainty and natural gas variability from the Sleipner field in [28]. Concentrations and ratios are relative to the respective background fluids; the stated ranges are for $c_{g,low,S_{max}}$ and $c_{g,high,S_{max}}$, respectively.

	$c_{g,low,S_{max}}$ **Low Captured CO_2 Values**	$c_{g,high,S_{max}}$ **High Captured CO_2 Values**	**Analytical Uncertainty**	**Variability in Natural Gas**	$c_{g,S_{max}}$ **rel. to Average Natural Gas**	$c_{g,S_{max}}$ **rel. to Atmosphere**	$c_{g,S_{max}}$ **rel. to Hydrates**
He	3.90E-05	3.92E-05	2%	8%	62–63%	744–749%	4,900,000%
^{4}He	3.90E-05	3.92E-05	2%	8%	62–63%	744–749%	-
^{3}He	5.86E-12	6.49E-12	3%	35%	62–68%	80–88%	-
^{3}He/^{4}He	1.50E-07	1.65E-07	3%	13%	104–115%	11–12%	-
Ar	5.22E-05	7.09E-05	2%	30%	166–225%	1%	52–71%
^{36}Ar	1.13E-07	1.75E-07	1%	45%	166–258%	1%	-
^{40}Ar	5.21E-05	7.07E-05	2%	30%	166–225%	1%	-
^{40}Ar/^{36}Ar	4.63E+02	4.05E+02	1%	5%	99–87%	156–137%	-
Kr	1.06E-08	1.16E-08	2%	18%	239–262%	1%	13–14%
^{84}Kr	8.12E-09	8.89E-09	2%	18%	239–261%	1%	-
^{86}Kr	2.46E-09	2.69E-09	1%	17%	239–262%	1%	-
^{86}Kr/^{84}Kr	3.03E-01	3.03E-01	1%	1%	100%	99%	-
Xe	6.36E-09	6.67E-09	5%	10%	458–480%	7–8%	13%
^{124}Xe	6.37E-12	7.46E-12	3%	8%	458–536%	8–9%	-
^{126}Xe	5.66E-12	6.67E-12	3%	11%	458–540%	7–9%	-
^{128}Xe	1.16E-10	1.38E-10	3%	17%	458–544%	7–8%	-
^{129}Xe	1.68E-09	1.98E-09	3%	11%	458–540%	7–9%	-
^{130}Xe	2.56E-10	3.03E-10	3%	12%	458–541%	7–9%	-
^{131}Xe	1.36E-09	1.60E-09	3%	10%	458–539%	7–9%	-
^{132}Xe	1.71E-09	2.02E-09	3%	9%	458–540%	7–9%	-
^{134}Xe	6.63E-10	7.82E-10	3%	11%	458–540%	7–9%	-
^{136}Xe	5.64E-10	6.65E-10	3%	11%	458–540%	7–9%	-
^{124}Xe/^{130}Xe	2.49E-02	2.46E-02	5%	9%	101–100%	106–105%	-
^{126}Xe/^{130}Xe	2.21E-02	2.20E-02	5%	3%	101%	101–101%	-
^{128}Xe/^{130}Xe	4.52E-01	4.55E-01	5%	5%	101–102%	96–96%	-
^{129}Xe/^{130}Xe	6.55E+00	6.54E+00	5%	1%	101%	101%	-
^{131}Xe/^{130}Xe	5.31E+00	5.30E+00	5%	2%	101%	102%	-
^{132}Xe/^{130}Xe	6.68E+00	6.67E+00	5%	1%	101%	101%	-
^{134}Xe/^{130}Xe	2.59E+00	2.58E+00	5%	1%	101%	101%	-
^{136}Xe/^{130}Xe	2.20E+00	2.20E+00	5%	1%	101%	101%	-

3.2. Tracer Addition

Needed concentrations in the injection stream to achieve additional distinction range from 1E-11 cm_{STP}^3/cm_{STP}^3 for some Xe isotopes to 1E-03 cm_{STP}^3/cm_{STP}^3 for elemental He. The results for the amounts of a specific gas isotope needed for deliberate tracer addition are shown in Table 4. Calculations are conducted in order to increase distinctiveness of the injected, equilibrating CO_2 from natural gas, following the description in Section 2.2. The results fulfill the condition set in Section 2.3. Then, the necessary concentrations

that the injected CO_2 needs to be labeled with to achieve the given concentrations after equilibration are given.

The necessary concentrations in the injected CO_2 are scaled up to volumes of the respective tracer gas needed in a $1MtCO_2/a$ storage project, depicting the large range of concentrations needed for the different gases. These volumes range from 1E+01 to 1E+08 l/a (Table 4). From the amounts needed, the cost of an isotope addition is derived to a wide range of 0.7 to 37,000 $US/tCO_2 for the different gases. For reference, the price calculation is performed to fulfill the method used in [18] (see Section 2.3). Here, tracer addition would be up to 3 orders of magnitude cheaper.

Table 4. Necessary noble gas concentrations in cm^3_{STP}/cm^3_{STP} and isotopic ratios to fulfill the detection condition described in Section 2.3 both in the equilibrated and the injected CO_2. For isotopic ratios, calculations are conducted for the isotope in the numerator of the ratio. As shown in Section 3.1, the distinctiveness condition for Xe and its isotopes is inherently met in our calculations. For Xe ratios, a concentration of 1.50E-11 ^{130}Xe inherent in the injected CO_2 is assumed. The volume is calculated for $1MtCO_2/a$ storage project, and the associated cost for a tracer addition is derived. For comparability, the cost is additionally derived with the method in [18] and gas prices as in [18], where applicable. Exchange rate used for prices in [18]: £ = 1.3·$US.

	Nec. Conc./ Ratio in Equilibrated CO_2	Nec. Conc. in Injected CO_2	Nec. Volume in a $1MtCO_2/a$ Project (l/a)	Gas Price ($US/l)	Cost ($US/tCO_2)	Cost; Method as in [18] ($US/tCO_2)	Gas Price Source
He	1.53E-04	1.26E-03	6.43E+08	57.2	37,000	18,000	[18]
^3He	3.02E-11	2.72E-10	1.39E+02	3800	0.69	750	[18]
$^3He/^4He$	7.72E-07	2.74E-10	1.40E+02	3800	0.69	0.07	[18]
Ar	1.43E-04	7.60E-04	3.88E+08	64.38	32,000	13,400	[18]
^{36}Ar	3.91E-07	2.09E-06	1.07E+06	1000	1066	450	Shell
$^{36}Ar/^{40}Ar$	3.79E-03	1.17E-06	5.97E+05	1000	597	23	Shell
Kr	1.50E-08	3.60E-08	1.84E+04	107	2.55	3.16	[18]
^{86}Kr	3.14E-09	5.55E-09	2.83E+03	1490	5.48	10.16	[18]
$^{86}Kr/^{84}Kr$	4.25E-01	1.08E-08	5.51E+03	1490	10.67	0.01	[18]
Xe	4.89E-09	Condition met inherently		340	-	3.13	[18]
$^{124}Xe/^{130}Xe$	8.48E-02	9.70E-11	4.95E+01	28,554	1.84	0.00026	[18]
$^{126}Xe/^{130}Xe$	6.21E-02	6.48E-11	3.31E+01	17,600	0.76	0.00014	[18]
$^{128}Xe/^{130}Xe$	1.35E+00	1.45E-09	7.40E+02	-	-	-	
$^{129}Xe/^{130}Xe$	1.63E+01	1.58E-08	8.06E+03	330	2.66	0.0062	Shell
$^{131}Xe/^{130}Xe$	1.44E+01	1.48E-09	7.55E+02	1650	1.25	0.0025	Shell
$^{132}Xe/^{130}Xe$	1.66E+01	1.60E-08	8.16E+03	2200	17.96	638	Shell
$^{134}Xe/^{130}Xe$	6.50E+00	6.33E-09	3.23E+03	4585	19.25	0.0044	[18]
$^{136}Xe/^{130}Xe$	5.55E+00	5.43E-09	2.77E+03	2200	6.09	0.0014	Shell

4. Discussion

4.1. Inherent Distinctiveness

The phase-partitioning calculations show that inherited noble gas signatures of injected CO_2 are significantly distinct compared with all background signatures, given the presented analytical uncertainty and database (Table 3). This is further demonstrated when mixing He, Ar, Kr, and Xe concentrations in the CO_2 with the respective gas concentrations in natural gas, atmosphere, and gas hydrates (yellow lines in Figure 2).
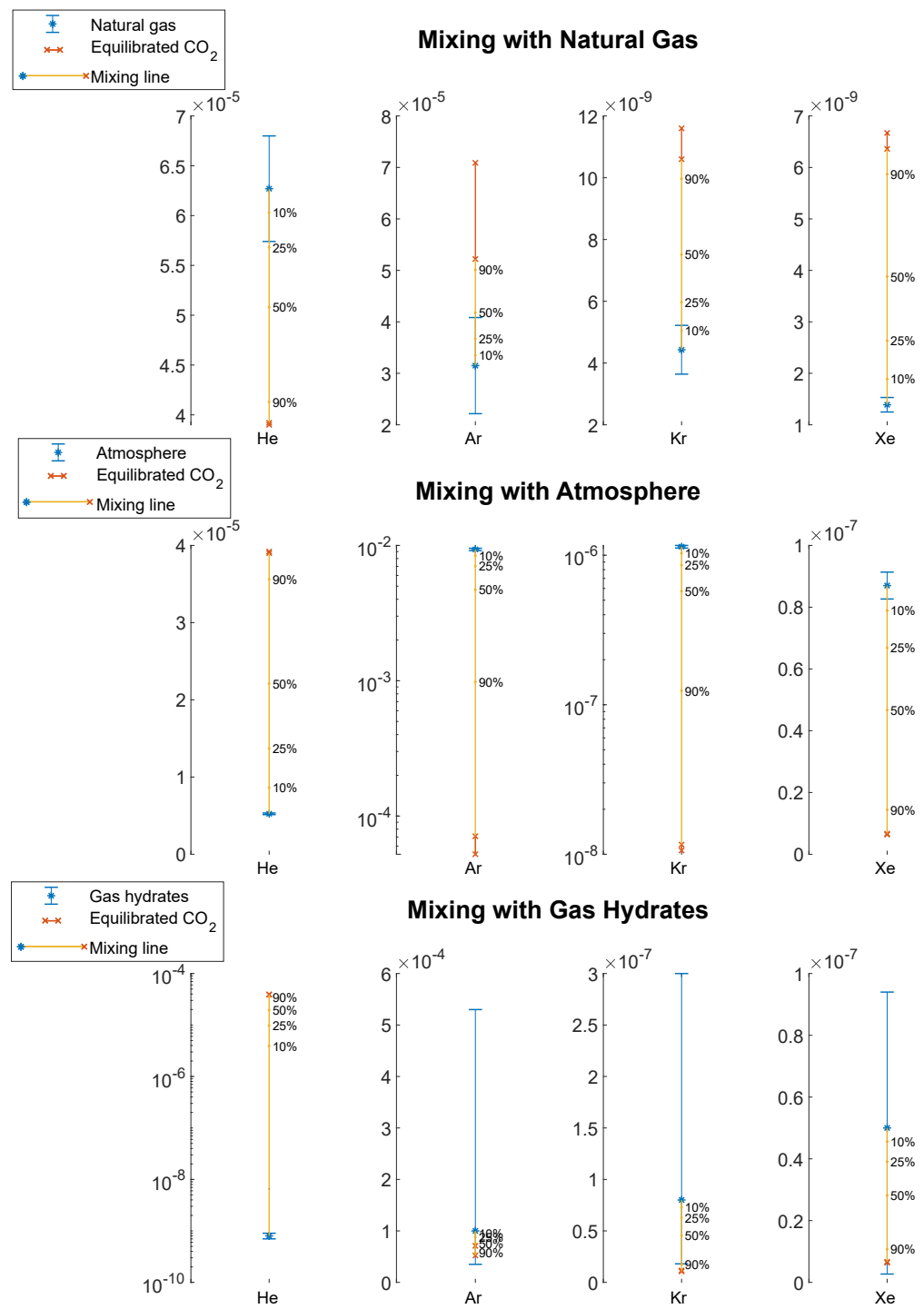
Figure 2. Mixing of the equilibrated CO_2 with background concentrations in natural gas, atmosphere, and gas hydrates in (cm^3_{STP}/cm^3_{STP}). For seawater, gas-specific solubilities have to be applied. The range of equilibrated CO_2 is the orange line, with the values as stated in Table 3. Mixing is calculated for the lower of these values. Background concentrations are shown with error bars (blue)—being dominated by the natural variability for natural gas and gas hydrates, and the analytical uncertainty for the atmosphere.

In the case of equilibrated CO_2 mixing with natural gas, case 2 in Figure 1, Xe is most distinct and would allow identification of injected CO_2 in gas mixtures at percentages of CO_2 as low as 3% (Figure 2). For He, Ar and Kr distinctiveness is worse. This is mainly caused by the natural variability in the natural gas (blue error bars in Figure 2). Further,

for Ar and Kr, the range of the concentrations in the equilibrated CO_2 is relatively large, resulting from the concentration range in the captured CO_2 (orange line in Figure 2).

Even though different to the natural gas, the equilibrated signature of injected CO_2 exhibits some characteristics of a radiogenic signature. Primarily, high He makes the signature very distinct compared to the atmosphere and gas hydrates (Figure 2). For mixing of injected and equilibrated CO_2 with the atmosphere, all gases are significantly different (note the logarithmic scale for Ar and Kr in the second row of Figure 2). He will be most reliable since He concentration is the only gas that is higher in the equilibrated CO_2 than in the atmosphere.

For seawater, the assumption can be made that the distinctiveness will be the same as for an atmospheric signature, considering that the same Henry's constants would be applied to the dissolution of noble gases for both air and leaking CO_2.

The very distinct depletion of He in gas hydrates allows unambiguous identification of an injected and equilibrated CO_2 component in a mixture of these two components (note the logarithmic scale for He in the third row of Figure 2). The other gases exhibit large natural variability and therefore do not add distinctiveness.

4.2. Limitations of the Method

4.2.1. Calculation Method

In the calculations of phase partitioning, we calculated the specific solubility in a CO_2-H_2O-system using the correction term of [20] (Equation (2)). For deriving the formation water concentrations of noble gases in the storage reservoir—currently not directly measured—we assumed equilibrium with the analyzed natural gas. Here, we used solubilities for a high-pressure H_2O-system, i.e., not applying κ_i in Equation (2). Such specific correction terms for the noble gas solubility in a CH_4-CO_2-system have yet to be derived. The CO_2-solubility correction, i.e., the preferential partitioning into the CO_2 phase, is exactly what makes Xe values in particular differ significantly (~500% in Table 3). Deriving correction terms for a high-pressure CH_4-CO_2-system may alter the concentrations and lead to the signatures that the injected CO_2 adopts to be less or more distinct. Further, impurities in the CO_2 injection stream could impact the applicability of solubilities for a pure CO_2-H_2O-system; however, such deviations are anticipated to be minor given the relatively pure nature of injected CO_2. For example, the injected CO_2 at the Sleipner storage site has a CH_4 constituent of only 1–2% [22].

We further assumed that phase partitioning is the only process influencing the signature before mixing. Mixing with native formation gases, such as minor CH_4 accumulations, could alter the mixtures significantly, i.e., including a signature of natural gas. Thereby, the injected CO_2 would be more similar to natural gas, reducing distinctiveness towards it. The inclusion of the radiogenic signature from native formation gases would, however, further increase distinctiveness towards shallow signatures.

4.2.2. Leakage Scenarios

Reaching initial equilibrium with the formation water may depend on the type of leakage. The later a leak occurs after injection, the more likely equilibrium is achieved. For "catastrophic" leakages—e.g., at the injection well—the CO_2 could stay in its depleted state (case (1) in Figure 1). Such a leak can be detected based on a suit of other geophysical and geochemical tools that are installed along the well [1]. The depleted noble gas concentrations could, however, be used for leakage attribution. For other advective leakage types—e.g., cases 2, 3, 4, and 5 in Figure 1—the CO_2 will likely have equilibrated during prior migration in the storage reservoir making our calculations applicable. This could also depend on leakage rates. Those have been constrained for natural CO_2 analogues [43], but it is unclear how that translates to other settings. Leakage for such fields showed that, for example, the elevated He concentrations are maintained up until the surface [44].

Our calculations assume full equilibration of the injected CO_2 with formation water. In [13], we argued that equilibrium is likely to be reached, considering that at the front

of a moving CO_2-plume, the concentration gradients between the two phases, formation water, and CO_2 are high. For a dedicated storage case, such a behavior was, for example, observed at Aquistore, where the injected CO_2 had adopted a radiogenic signature one year after injection [11]. In contrast, the formation water of a system that is continuously flushed may become depleted in the noble gases over time, leading to domination of the depleted, original signature of the captured CO_2. Such a behavior was observed for the specific case of the Cranfield EOR field [16]. Although, in that case, the presence of a hydrocarbon phase meant low residual water saturation and a limited volume of water in contact with the CO_2 phase, leading to more rapid noble gas stripping than would be observed for CO_2 storage in saline aquifers.

In the phase-partitioning and subsequent mixing calculations, the dissolution of CO_2 into the brine over time is not taken into account. This effect would tend to increase the residual noble gas concentrations and reduce the gas water volume ratio, V_g/V_{H_2O}. Our calculations do not evaluate the migration of a dissolved CO_2 phase. It is known (from natural analogues) that ex-solution of dissolved CO_2 tends to lead to quantitative partitioning of the dissolved noble gas load into the CO_2 phase and, thus, the reservoir signature is likely to be inherited [44]. However, the complexities of multistage dissolution–ex-solution have not been assessed in this study, and further investigation of the preservation of the noble gas signature in such systems is merited.

4.2.3. Mixing Calculations

Mixing calculations of end-members will not allow the complete exclusion of a minor contribution of one end-member to a mixture, due to analytical uncertainty typically being an unsystematic error in the sample measurement [45]. Further, noble gases are found in every natural system and exhibit significant natural concentration variability, thereby introducing uncertainty in end-member calculations. The use of element or isotope ratios helps to reduce this uncertainty in mixing calculations because of the covariance of element or isotope concentrations, which removes dilution or concentration effects that otherwise create variability in absolute element concentrations. Further, the calculations become more constrained the more accurately the end-member compositions are known from baseline characterization of the storage system or via measurements of the captured and injected CO_2. For example, above hydrocarbon systems, methane releases may imprint fluids in seafloor sediments with a radiogenic signature, reducing the distinctiveness of leaking CO_2 into the surrounding environment (Figure 1). Further, the gas hydrates composition is only known for the element and not the isotopic ratios, resulting in an incomplete description of one possible end-member.

Despite these uncertainties, noble gas signatures will deliver strong evidence when analyzing the fluids of a potential leak, as our calculations have shown. In Figure 2, only one element was used. By combining the analysis of a number of isotopes or ratios, the vector of the mixing line representing possible solutions to the mixing calculation increases; thereby, measurement errors become less influential. This is exemplified for a mixing with natural gas, where using both Kr and Xe increases differentiability (Figure 3a). Meanwhile, for atmosphere, the inclusion of the ^{3}He/^{4}He ratio has the same effect. Besides, noble gases such as this could include additional geochemical constraints, such as the stable isotopic composition of the CO_2. For example, injected CO_2 with an atmospheric ^{13}C isotope signature provides an additional distinct parameter with which to discriminate the CO_2 from natural gas [6].
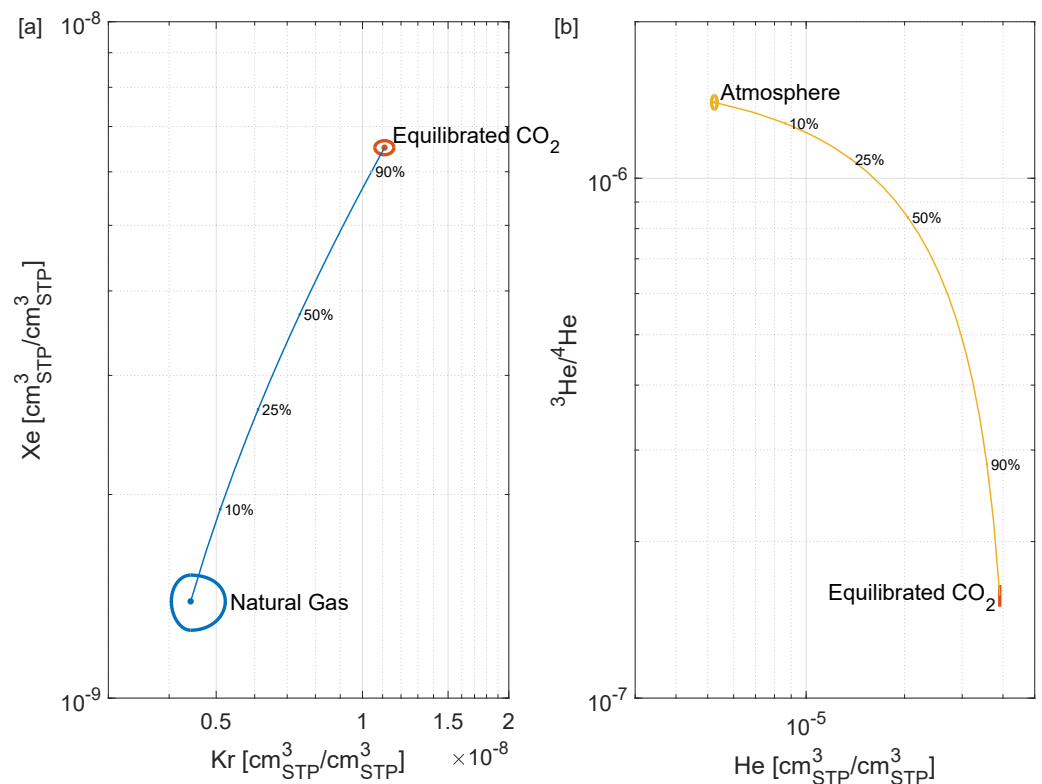
Figure 3. Increasing the dimension of included isotopes/ratios increases differentiability. (**a**) Mixing with natural gas using both Kr and Xe. (**b**) Mixing with the atmosphere including ^{3}He/^{4}He. The mean concentration is surrounded by the respective error ellipses.

A further approach to reduce uncertainty introduced by natural variability is the addition of artificial tracers, e.g., SF_6 or PFCs. Since these are not present in the natural environment, uncertainties are reduced to the analytical uncertainty alone. Partly, however, these tracers have other disadvantages, such as toxicity or functionality as a greenhouse gas [18]. For details and examples, the reader may be referred to [15,18], where the addition of artificial trace gases is also analyzed from a cost perspective.

4.3. Tracer Addition

Tracer addition could help to manage the limitations of the calculation, as described in the previous Section 4.2, i.e., increase the altering of the injected CO_2 signature of a mixture against the natural variability and the analytical uncertainty. The additional distinction through the addition is depicted for Xe and ^{126}Xe/^{130}Xe in Figure 4.

The necessary concentrations to be added into the injection stream are lowest for ^{3}He and ^{124,126}Xe isotopes with concentrations of ∼1E-10 cm^3_{STP}/cm^3_{STP} or of 50–100 l/$MtCO_2$. These He and Xe isotopes are among the most expensive in terms of cost per liter, at 1000–10,000 \$US/l (Table 4). Despite this, due to the small amounts required, these would be the cheapest tracers to add with a cost of ∼0.7 \$US/tCO_2 (Table 4).

Xe tracer addition appears to be the most suitable noble gas tracer in CO_2 storage, as both lab and field experiments suggest that Xe could even have an early warning function, in contrast to He [46,47]. This is due to the molecule size, i.e., allowing He to enter smaller, dead-end pores and thereby getting retarded. Adding ^{3}He would also shift the ^{3}He/^{4}He ratio towards atmospheric values, thereby interfering with the distinction to atmospheric signatures. Further, ^{3}He has seen a price increase and supply shortage in the last decades [48] that may make its application unfeasible within a few decades. In contrast, availability of Xe isotopes is estimated to be sufficient [15].
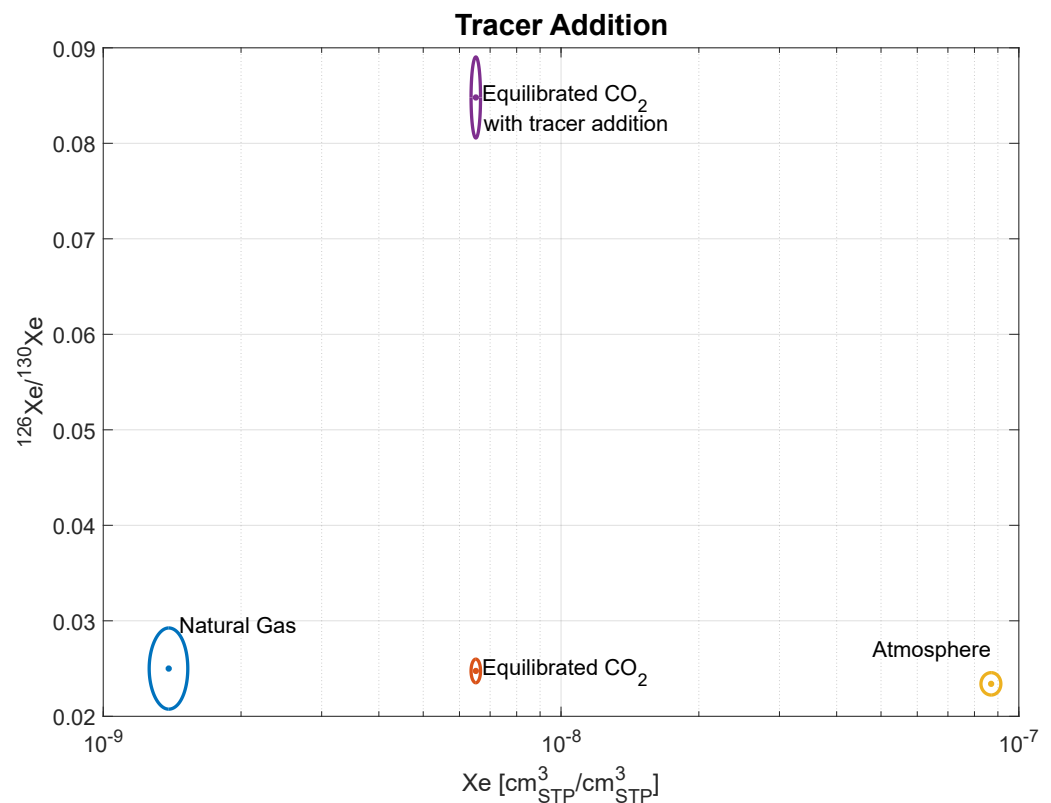
Tracer Addition

Figure 4. The impact of tracer addition: The signatures of natural gas, equilibrated CO_2, and atmosphere in comparison to the equilibrated CO_2 with tracer addition. The mean concentration is surrounded by the respective error ellipses.

The cheapest tracer addition would cost $\sim$0.7 \$US/tCO_2, given our assumptions. In comparison to the cost of noble gas tracer addition derived with the method in [18], i.e., "10 times the detectable perturbation above background levels", the cost estimates derived in our study are typically higher (Table 4). Even though the same isotopes are assigned the lowest cost in the derivation of [18], the cost presented here is several orders of magnitude more expensive, e.g., for ^{126}Xe 0.00014 \$US/tCO_2 after the method in [18] vs. 0.76 \$US/tCO_2 for the derivation presented here. Our results are also higher, but more in line with calculations for detection in soil gas made in [15], which resulted in a cost of $\sim$0.1 \$US/tCO_2 for both ^{3}He and ^{136}Xe.

Our criterion for distinctiveness of CO_2 in leakage detection schemes and considering the phase partitioning estimates leads to higher volumes of tracers needed and increased costs compared to previous studies [15,18]. However, defining when a signature is sufficiently distinct is, to a certain degree, a subjective choice. It appears that this will have to be defined by decision makers, i.e., how soon and how certain one wants to know a leakage/contamination in a trade-off between cost and risk.

In comparison to total operational costs of a CCS project, $\sim$0.7 \$US/tCO_2 is a low cost, for example, compared to a CO_2 capture cost of 15–120 \$US/tCO_2 [49]. However, considering that the current cost of the whole monitoring scheme of running sites is in the order of 1–4 \$US/a [1], the added cost would be a significant contribution to the total monitoring cost, especially considering the generally low leakage likelihood [50]. Further, on the one hand the estimated cost does not yet include sampling, analysis, and evaluation costs, on the other hand there may be a price reduction through bulk orders of the respective tracer gas.

4.4. Technical Aspects of Tracer Addition

The addition of a noble gas tracer into a CO_2 injection stream represents an impurity, which potentially changes the thermodynamic properties of the CO_2. Even though indi-

vidual for each CO_2-tracer mixture, depending on the type and amount of an impurity, typically, the critical pressure is increased [51]. This implies changes of the transport properties and could affect transportation and injection setup, and is thus likely to add costs. Impurities also tend to decrease the viscosity of the fluid mixture [51], reducing migration properties of the CO_2 in the reservoir. Therefore, it seems desirable to have the lowest concentrations of the added tracer as possible. For the trace isotopes we derive as most economical, i.e., elemental He and Ar being excluded, the added impurity is very low (below 1E-06 vol%) compared to those typically found after the CO_2 capture process, such as N_2, O_2, H_2S, and H_2O which can collectively make up 1–5 vol%) [52].

On another technical note, achieving continuous tracer concentrations in a gas stream as low as 1E-11–1E-10 cm^3_{STP}/cm^3_{STP} is not trivial. Nimz and Hudson [15] outline how a side-track with flow regulation and an additional compressor could be used. It is also suggested that the low volumes of the gas necessary, e.g., tenths of liter per year, could better be applied through prior mixture with CO_2 as the carrier gas, i.e., stepwise dilution [15]. It might also be considered to have pulsed injection patterns and assume effective distribution after injection.

4.5. Noble Gases in Monitoring Schemes

In case of an observed or suspected CO_2 anomaly or leakage, noble gases are very likely to give an indication of the CO_2 source due to the distinct signatures in the environment. Therefore, noble gases' main application will—also offshore—lie in leakage attribution as it has in the past, e.g., [14].

In contrast, high-frequency monitoring of a storage site for leakage detection, does seem less attractive given that noble gas analysis for high sensitivity, precision, and accuracy—i.e., full isotopic analysis including the least abundant isotopes—currently has to be conducted using a lab-based multicollector mass spectrometers with a cost of up to several thousand $US per sample. Further, collecting and transporting a sample to the lab does introduce a significant time lag between sampling and interpreting results.

However, in recent years, in situ, continuous, and remotely controllable noble gas analysers have been developed [53,54]. Currently these techniques cannot deliver full isotopic resolution, typically covering the most abundant elements of a noble gas, e.g., ^{4}He, but not ^{3}He. Further, the limit of quantification is usually in the ppm range. Still, with on-site measurements, not only leakage attribution but also leakage detection may become possible. Especially, the elevated concentrations of He (see Table 3) could be targeted with a mobile mass spectrometer when sampling offshore seabed fluid releases, as demonstrated in the vicinity of black smokers [53]. Both water and gas analysis could be conducted on board a ship to scan if elevated He concentrations indicate leaking CO_2 from a deep CO_2 source with a radiogenic signature. Simultaneous measurement of O_2, N_2, CH_4, and CO_2, which the instrument is capable of, add valuable information.

In contrast to the previous case, the application of these technologies for the monitoring of the production stream at an operating gas field is limited. Considering our results, e.g., for the mixture of CO_2 and natural gas, where Xe is the most distinctive gas, the portable analysis systems do currently not deliver sufficient sensitivity for detection of Xe concentrations of 1E-09 cm^3_{STP}/cm^3_{STP}, even with tracer addition (see Table 3). Further advances of these technologies may allow for wider applicability and for continuous, remote leakage detection.

5. Conclusions

The partitioning of the formation water noble gas signature into injected CO_2 is destined to allow the differentiation from natural geological fluids or gases due to the specific fractionation through the phase partitioning in a CO_2-H_2O-system. Meanwhile, there are uncertainties attached to the distinction towards natural gas, i.e., unknown solubilities in a CH_4-H_2O-system, the difference between the adopted radiogenic signature and that of shallow signatures is very pronounced.

The presented approach also allows us to evaluate the active addition of a noble gas tracer to the injection stream with the goal of maintaining a significantly different noble gas signature after the equilibration. Xe isotopes are the most relevant choice for noble gas tracer addition, since they have the lowest concentrations in the background (see Table 1) and do not impact the main features of the radiogenic signature, in contrast to He. Such an addition will increase identifiability but adds significant cost to a monitoring scheme of a storage project.

Further, baseline characterization is fundamental, and even though we use relevant analogues in this study, each storage site and CO_2 capture plant has to be expected to be different. For the inherent recognition through Xe, specific fractionation patterns in captured CO_2, such as elevated Kr and Xe at oxyfuel plants, could significantly increase detectability. Further, formation water concentrations are only indirectly derived.

Considering that CCS is currently only feasible with government subsidies, adding cost to CCS projects endangers its large-scale application [3]. Therefore, implementation of a noble gas tracer addition and other MMV methods will, on the one hand, depend on the legal framework regarding long-term liability of safe containment, and on the other hand, on widespread and meaningful implementation of carbon pricing options, such as carbon taxes or a carbon trading system. Further, (i) with the involved techniques maturing over the past and coming decades, uncertainties attached to such advanced green investments should reduce and thereby improve the green finance framework [55]; (ii) and increased MMV expenditures could increase the environmental reputation of the involved entities [55].

The planned, continuous MMV program in the Norwegian storage project 'Longship' currently does not include noble gases [27]. We believe that noble gas sampling should be considered during routine environmental surveys and should definitely be the content of 'triggered' environmental monitoring surveys. The content of such a triggered environmental monitoring survey has yet to be defined.

This work is another step towards upscaling and realizing the utilization of noble gas tracers, quantitatively and qualitatively describing how noble gases can be applied, which behavior is to be expected, and how they may be useful in deploying CCS. Implementation in case-specific leakage models, including secondary processes such as dissolution and mineralization of CO_2 combined with advances in defining solubilities of noble gases in the relevant systems and further developments in field-applicable measurement devices, will constrain our findings further and allow for wider application of noble gases in monitoring schemes for CO_2 storage sites, enhancing detectability and source attribution.

References

1. IEAGHG. Monitoring and Modelling of CO_2 Storage: The Potential for Improving the Cost-Benefit Ratio of Reducing Risk, 2020-01. Available online: https://climit.no/wp-content/uploads/sites/4/2020/05/2020-01-Monitoring-and-Modelling-of-CO2-Storage.pdf (accessed on 2 April 2021).

2.   Ringrose, P. *How to Store* CO₂ *Underground: Insights from Early-Mover CCS Projects*; Springer Nature Switzerland AG: Cham, Switzerland, 2020.

3.   Hongo, T. Carbon Pricing to Promote Green Energy Projects. In *Handbook of Green Finance*; Springer: Singapore, 2019; pp. 157–181. [CrossRef]

4.   Myers, M.; Stalker, L.; Pejcic, B.; Ross, A. Tracers—Past, present and future applications in CO₂ geosequestration. *Appl. Geochem.* **2013**, *30*, 125–135. [CrossRef]

5.   Holland, G.; Gilfillan, S. Application of Noble Gases to the Viability of CO₂ Storage. In *The Noble Gases as Geochemical Tracers*; Springer: Berlin/Heidelberg, Germany, 2012; pp. 177–223._8. [CrossRef]

6.   Flude, S.; Johnson, G.; Gilfillan, S.M.V.; Haszeldine, R.S. Inherent Tracers for Carbon Capture and Storage in Sedimentary Formations: Composition and Applications. *Environ. Sci. Technol.* **2016**, *50*, 7939–7955. [CrossRef]

7.   Sano, Y.; Marty, B.; Burnard, P. Noble Gases in the Atmosphere. In *Advances in Isotope Geochemistry*; Springer: Berlin/Heidelberg, Germany, 2013; pp. 17–31. [CrossRef]

8.   Ballentine, C.J.; Burnard, P.G. Production, Release and Transport of Noble Gases in the Continental Crust. *Rev. Mineral. Geochem.* **2002**, *47*, 481–538. [CrossRef]

9.   Moreira, M.A.; Kurz, M.D. Noble Gases as Tracers of Mantle Processes and Magmatic Degassing. In *Advances in Isotope Geochemistry*; Springer: Berlin/Heidelberg, Germany, 2013; pp. 371–391. [CrossRef]

10.   Burnard, P. (Ed.) *The Noble Gases as Geochemical Tracers*; Springer: Berlin/Heidelberg, Germany, 2013. [CrossRef]

11.   Flude, S.; Györe, D.; Stuart, F.; Zurakowska, M.; Boyce, A.; Haszeldine, R.; Chalaturnyk, R.; Gilfillan, S. The inherent tracer fingerprint of captured CO₂. *Int. J. Greenh. Gas Control* **2017**, *65*, 40–54. [CrossRef]

12.   Weber, U.W.; Kipfer, R.; Horstmann, E.; Ringrose, P.; Kampman, N.; Tomonaga, Y.; Brennwald, M.S.; Sundal, A. Noble gas tracers in gas streams at Norwegian CO₂ capture plants. *Int. J. Greenh. Gas Control* **2021**, *106*, 103238. [CrossRef]

13.   Weber, U.; Kampman, N.; Mikoviny, T.; Thomassen, J.; Sundal, A. Noble Gases as Monitoring Tracers in CCS: A Case Study with CO₂ from the Waste-to-Energy Plant Klemetsrud, Norway. *SSRN Electron. J.* **2021**. [CrossRef]

14.   Gilfillan, S.M.; Sherk, G.W.; Poreda, R.J.; Haszeldine, R.S. Using noble gas fingerprints at the Kerr Farm to assess CO₂ leakage allegations linked to the Weyburn-Midale CO₂ monitoring and storage project. *Int. J. Greenh. Gas Control* **2017**, *63*, 215–225. [CrossRef]

15.   Nimz, G.; Hudson, G. The Use of Noble Gas Isotopes for Monitoring Leakage of Geologically Stored CO₂. In *Carbon Dioxide Capture for Storage in Deep Geologic Formations—Results from the* CO₂ *Storage Project, 0-08-044570-5*; Elsevier: Oxford, UK, 2005; Volume 2.

16.   Györe, D.; Stuart, F.M.; Gilfillan, S.M.; Waldron, S. Tracing injected CO₂ in the Cranfield enhanced oil recovery field (MS, USA) using He, Ne and Ar isotopes. *Int. J. Greenh. Gas Control* **2015**, *42*, 554–561. [CrossRef]

17.   Györe, D.; Gilfillan, S.M.; Stuart, F.M. Tracking the interaction between injected CO₂ and reservoir fluids using noble gas isotopes in an analogue of large-scale carbon capture and storage. *Appl. Geochem.* **2017**, *78*, 116–128. [CrossRef]

18.   Roberts, J.J.; Gilfillan, S.M.; Stalker, L.; Naylor, M. Geochemical tracers for monitoring offshore CO₂ stores. *Int. J. Greenh. Gas Control* **2017**, *65*, 218–234. [CrossRef]

19.   Ju, Y.; Lee, S.S.; Kaown, D.; Lee, K.K.; Gilfillan, S.M.; Hahm, D.; Park, K. Noble gas as a proxy to understand the evolutionary path of migrated CO₂ in a shallow aquifer system. *Appl. Geochem.* **2020**, *118*, 104609. [CrossRef]

20.   Warr, O.; Rochelle, C.A.; Masters, A.; Ballentine, C.J. Determining noble gas partitioning within a CO₂–H₂O system at elevated temperatures and pressures. *Geochim. Cosmochim. Acta* **2015**, *159*, 112–125. [CrossRef]

21.   Prinzhofer, A. Noble Gases in Oil and Gas Accumulations. In *The Noble Gases as Geochemical Tracers*; Springer: Berlin/Heidelberg, Germany, 2013; pp. 225–247. [CrossRef]

22.   Chadwick, R.; Eiken, O. Offshore CO₂ storage: Sleipner natural gas field beneath the North Sea. In *Geological Storage of Carbon Dioxide* CO₂; Woodhead Publishing: Cambridge, UK, 2013; pp. 227–253. [CrossRef]

23.   Hansen, O.; Gilding, D.; Nazarian, B.; Osdal, B.; Ringrose, P.; Kristoffersen, J.B.; Eiken, O.; Hansen, H. Snøhvit: The History of Injecting and Storing 1 MtCO₂ in the Fluvial Tubåen Fm. *Energy Procedia* **2013**, *37*, 3565–3573. [CrossRef]

24.   Halland, E.; Riis, F.; Mujezinović, J. (Eds.) *CO₂ Storage Atlas Norwegian Continental Shelf*; Norwegian Petroleum Directorate: Stavanger, Norway, 2014.

25.   IEA Greenhouse Gas R&D Programme (IEA GHG). *Remediation of Leakage form* CO₂ *Storage Reservoirs, 2007/11*; IEA Greenhouse R&D Programme: Stoke Orchard, UK, 2007.

26.   The Full-Scale CCS Project in Norway. Available online: www.ccsnorway.com (accessed on 9 April 2021).

27.   Furre, A.K.; Meneguolo, R.; Pinturier, L.; Bakke, K. Planning deep subsurface CO₂ storage monitoring for the Norwegian full-scale CCS project. *First Break* **2020**, *38*, 55–60. [CrossRef]

28.   Barry, P.; Lawson, M.; Meurer, W.; Warr, O.; Mabry, J.; Byrne, D.; Ballentine, C. Noble gases solubility models of hydrocarbon charge mechanism in the Sleipner Vest gas field. *Geochim. Cosmochim. Acta* **2016**, *194*, 291–309. [CrossRef]

29.   Ballentine, C.; O'Nions, R.; Coleman, M. A Magnus opus: Helium, neon, and argon isotopes in a North Sea oilfield. *Geochim. Cosmochim. Acta* **1996**, *60*, 831–849. [CrossRef]

30.   Ballentine, C.J.; Schoell, M.; Coleman, D.; Cain, B.A. 300-Myr-old magmatic CO₂ in natural gas reservoirs of the west Texas Permian basin. *Nature* **2001**, *409*, 327–331. [CrossRef] [PubMed]

31.   Gilfillan, S.M.; Ballentine, C.J.; Holland, G.; Blagburn, D.; Lollar, B.S.; Stevens, S.; Schoell, M. Cassidy, M. The noble gas geochemistry of natural CO_2 gas reservoirs from the Colorado Plateau and Rocky Mountain provinces, USA. *Geochim. Cosmochim. Acta* **2008**, *72*, 1174–1198. [CrossRef]

32.   Tomonaga, Y.; Brennwald, M.S.; Kipfer, R. Using helium and other noble gases in ocean sediments to characterize active methane seepage off the coast of New Zealand. *Mar. Geol.* **2013**, *344*, 34–40. [CrossRef]

33.   Nuzzo, M.; Tomonaga, Y.; Schmidt, M.; Valadares, V.; Faber, E.; Piñero, E.; Reitz, A.; Haeckel, M.; Tyroller, L.; Godinho, E.; et al. Formation and migration of hydrocarbons in deeply buried sediments of the Gulf of Cadiz convergent plate boundary—Insights from the hydrocarbon and helium isotope geochemistry of mud volcano fluids. *Mar. Geol.* **2019**, *410*, 56–69. [CrossRef]

34.   Winckler, G.; Aeschbach-Hertig, W.; Holocher, J.; Kipfer, R.; Levin, I.; Poss, C.; Rehder, G.; Suess, E.; Schlosser, P. Noble gases and radiocarbon in natural gas hydrates. *Geophys. Res. Lett.* **2002**, *29*, 63-1–63-4. [CrossRef]

35.   Sano, Y.; Takahata, N. Measurement of Noble Gas Solubility in Seawater Using a Quadrupole Mass Spectrometer. *J. Oceanogr.* **2005**, *61*, 465–473. [CrossRef]

36.   Horstad, I.; Larter, S.R. Petroleum Migration, Alteration, and Remigration Within Troll Field, Norwegian North Sea. *AAPG Bulletin* **1997**, *81*. [CrossRef]

37.   Horstmann, E.; Tomonaga, Y.; Brennwald, M.; Schmidt, M.; Liebetrau, V.; Kipfer, R. Noble gases in sediment pore water yield insights into hydrothermal fluid transport in the northern Guaymas Basin. *Mar. Geol.* **2021**, *434*, 106419. [CrossRef]

38.   Mazzini, A.; Svensen, H.; Planke, S.; Forsberg, C.; Tjelta, T. Pockmarks and methanogenic carbonates above the giant Troll gas field in the Norwegian North Sea. *Mar. Geol.* **2016**, *373*, 26–38. [CrossRef]

39.   Ballentine, C.J.; Burgess, R.; Marty, B. Tracing Fluid Origin, Transport and Interaction in the Crust. *Rev. Mineral. Geochem.* **2002**, *47*, 539–614. [CrossRef]

40.   Ouyang, L.B. New Correlations for Predicting the Density and Viscosity of Supercritical Carbon Dioxide Under Conditions Expected in Carbon Capture and Sequestration Operations. *Open Pet. Eng. J.* **2011**, *5*, 13–21. [CrossRef]

41.   NIST. Thermophysical Properties of Fluid Systems. Available online: https://webbook.nist.gov/chemistry/fluid/ (accessed on 2 November 2020).

42.   Burnside, N.; Naylor, M. Review and implications of relative permeability of CO_2/brine systems and residual trapping of CO_2. *Int. J. Greenh. Gas Control* **2014**, *23*, 1–11. [CrossRef]

43.   Miocic, J.M.; Gilfillan, S.M.V.; Frank, N.; Schroeder-Ritzrau, A.; Burnside, N.M.; Haszeldine, R.S. 420,000 year assessment of fault leakage rates shows geological carbon storage is secure. *Sci. Rep.* **2019**, *9*, 1–9. [CrossRef]

44.   Wilkinson, M.; Gilfillan, S.V.M.; Haszeldine, R.S.; Ballentine, C.J. Plumbing the depths: Testing natural tracers of subsurface CO_2 origin and migration, Utah. *Carbon Dioxide Sequestration Geol. Media—State Sci. AAPG Stud. Geol.* **2009**, *59*, 619–634. [CrossRef]

45.   Weltje, G.J. End-member modeling of compositional data: Numerical-statistical algorithms for solving the explicit mixing problem. *Math. Geol.* **1997**, *29*, 503–549. [CrossRef]

46.   Carrigan, C.R.; Heinle, R.A.; Hudson, G.B.; Nitao, J.J.; Zucca, J.J. Trace gas emissions on geological faults as indicators of underground nuclear testing. *Nature* **1996**, *382*, 528–531. [CrossRef]

47.   Kilgallon, R.; Gilfillan, S.; Edlmann, K.; McDermott, C.; Naylor, M.; Haszeldine, R. Experimental determination of noble gases and SF_6, as tracers of CO_2 flow through porous sandstone. *Chem. Geol.* **2018**, *480*, 93–104. [CrossRef]

48.   Cho, A. Helium-3 Shortage Could Put Freeze On Low-Temperature Research. *Science* **2009**, *326*, 778–779. [CrossRef] [PubMed]

49.   IEA. Levelised Cost of CO_2 Capture by Sector and Initial CO_2 Concentration. 2019. Available online: https://www.iea.org/data-and-statistics/charts/levelised-cost-of-co2-capture-by-sector-and-initial-co2-concentration-2019 (accessed on 6 April 2021).

50.   Alcalde, J.; Flude, S.; Wilkinson, M.; Johnson, G.; Edlmann, K.; Bond, C.E.; Scott, V.; Gilfillan, S.M.V.; Ogaya, X.; Haszeldine, R.S. Estimating geological CO_2 storage security to deliver on climate mitigation. *Nat. Commun.* **2018**, *9*. [CrossRef] [PubMed]

51.   Al-Siyabi, I. Effect of Impurities on CO_2 Stream Properties. Ph.D. Thesis, Heriot-Watt University, Edinburgh, UK, 2013.

52.   Porter, R.T.; Fairweather, M.; Pourkashanian, M.; Woolley, R.M. The range and level of impurities in CO_2 streams from different carbon capture sources. *Int. J. Greenh. Gas Control* **2015**, *36*, 161–174. [CrossRef]

53.   Brennwald, M.S.; Schmidt, M.; Oser, J.; Kipfer, R. A Portable and Autonomous Mass Spectrometric System for On-Site Environmental Gas Analysis. *Environ. Sci. Technol.* **2016**, *50*, 13455–13463. [CrossRef] [PubMed]

54.   Chatton, E.; Labasque, T.; de La Bernardie, J.; Guihéneuf, N.; Bour, O.; Aquilina, L. Field Continuous Measurement of Dissolved Gases with a CF-MIMS: Applications to the Physics and Biogeochemistry of Groundwater Flow. *Environ. Sci. Technol.* **2016**, *51*, 846–854. [CrossRef] [PubMed]

55.   Falcone, P.M. Environmental regulation and green investments: The role of green finance. *Int. J. Green Econ.* **2020**, *14*, 159. [CrossRef]